Water Research 256 (2024) 121616

Contents lists available at ScienceDirect

Water Research

journal homepage: www.elsevier.com/locate/watres

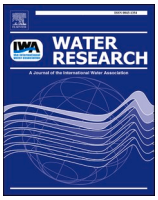

Enhancing bioelectrochemical hydrogen production from industrial wastewater using Ni-foam cathodes in a microbial electrolysis cell pilot plant

Oscar Guerrero-Sodric, Juan Antonio Baeza *, Albert Guisasola

GENOCOV, Department of Chemical, Biological and Environmental Engineering, School of Engineering, Universitat Autònoma de Barcelona, Bellaterra 08193, Spain

ARTICLE INFO

Keywords:
Bioelectrochemical systems
Hydrogen
Microbial electrolysis cell
Pilot scale
Wastewater treatment

ABSTRACT

Microbial electrolysis cells (MECs) have garnered significant attention as a promising solution for industrial wastewater treatment, enabling the simultaneous degradation of organic compounds and biohydrogen production. Developing efficient and cost-effective cathodes to drive the hydrogen evolution reaction is central to the success of MECs as a sustainable technology. While numerous lab-scale experiments have been conducted to investigate different cathode materials, the transition to pilot-scale applications remains limited, leaving the actual performance of these scaled-up cathodes largely unknown. In this study, nickel-foam and stainless-steel wool cathodes were employed as catalysts to critically assess hydrogen production in a 150 L MEC pilot plant treating sugar-based industrial wastewater. Continuous hydrogen production was achieved in the reactor for more than 80 days, with a maximum COD removal efficiency of 40 %. Nickel-foam cathodes significantly enhanced hydrogen production and energy efficiency at non-limiting substrate concentration, yielding the maximum hydrogen production ever reported at pilot-scale (19.07 ± 0.46 L H_2 m^{-2} d^{-1} and 0.21 ± 0.01 m^3 m^{-3} d^{-1}). This is a 3.0-fold improve in hydrogen production compared to the previous stainless-steel wool cathode. On the other hand, the higher price of Ni-foam compared to stainless-steel should also be considered, which may constrain its use in real applications. By carefully analysing the energy balance of the system, this study demonstrates that MECs have the potential to be net energy producers, in addition to effectively oxidize organic matter in wastewater. While higher applied potentials led to increased energy requirements, they also resulted in enhanced hydrogen production. For our system, a conservative applied potential range from 0.9 to 1.0 V was found to be optimal. Finally, the microbial community established on the anode was found to be a syntrophic consortium of exoelectrogenic and fermentative bacteria, predominantly *Geobacter* and *Bacteroides*, which appeared to be well-suited to transform complex organic matter into hydrogen.

1. Introduction

The urgent need for sustainable waste management practices and the increasing interest in energy recovery have encouraged the exploration of energy-from-waste technologies. Among the plethora of opportunities to recover energy from wastes, wastewater treatment has emerged as a promising research field (Kollmann et al., 2017). Simultaneous treatment of wastewater and energy harnessing presents several advantages for a more sustainable future. Among the existing methods for energy recovery from wastewater, anaerobic digestion for biogas production stands out as the most widely adopted approach (Obileke et al., 2021). However, other promising alternatives focus on generating green hydrogen as an energy carrier (Guo et al., 2019). Hydrogen has a higher energy content per unit mass compared to biogas and contributes to reducing the carbon footprint. Furthermore, it can be applied in a wide range of processes beyond being a fuel as it is a valuable feedstock for many industrial processes. Thus, hydrogen as a clean energy carrier has gained significant global interest (El-Emam and Özcan, 2019). Conventional technologies for hydrogen production, such as natural gas reforming or water electrolysis, face cost competitiveness and sustainability challenges. Consequently, the biological approach emerges as a promising alternative to tackle these limitations (Singh and Das, 2019; Younas et al., 2022). The most common biological technologies such as photofermentation, dark fermentation or microbial electrolysis cells

* Corresponding author.
E-mail address: JuanAntonio.Baeza@uab.cat (J.A. Baeza).

https://doi.org/10.1016/j.watres.2024.121616
Received 24 December 2023; Received in revised form 25 March 2024; Accepted 14 April 2024
Available online 16 April 2024

(MECs) employ microorganisms and enzymes as biocatalysts.

In MECs, electrochemistry is combined with the metabolism of electroactive microorganisms aiming at converting organic substrates into valuable hydrogen (Liu et al., 2005). These microorganisms, called exoelectrogens, present the unique ability to donate the electrons released during their metabolic processes to an external electrode (Logan, 2008). Exoelectrogens form biofilms on the anode, where they oxidize organic matter and release electrons. These electrons then travel through an electrical circuit from the anode to the cathode, ultimately contributing to the cathodic hydrogen evolution reaction (HER). However, HER does not occur spontaneously and requires the addition of a certain energy in form of applied potential (ΔV). In accordance with the Nernst equation, a theoretical ΔV of 0.13 V is required (considering acetate as electron donor, pH = 7 and standard conditions). This theoretical potential is remarkably lower, by an order of magnitude, compared to the theoretical ΔV to drive water electrolysis under the same conditions. Considering these low energy requirements and the estimated amount of energy present in wastewaters (approximately 15 kJ g^{-1} COD), MECs could ideally recover in form of hydrogen gas more than 10 times the energy needed to treat this wastewater under the current conventional treatments.

However, in practice, the energy requirements of MECs to produce hydrogen are significantly higher than the theoretical ones. The need of a membrane, along with the anode and cathode overpotentials, contribute significantly to the voltage losses (Sleutels et al., 2009a). Therefore, the required applied potential usually ranges from 0.6 to 1.0 V, which decreases the process energy efficiency to a certain extent (Guisasola et al., 2020). These voltages are still much lower than those reported for abiotic water electrolysis, which commonly range from 1.8 to 2.4 V (Carmo et al., 2013), positioning MECs as a more sustainable alternative for hydrogen production. Lab-scale MECs have yielded high hydrogen production rates (1–10 m^3 H_2 m^{-3} reactor d^{-1}) (Guisasola et al., 2020) that would make this technology viable if achieved at pilot scale, although additional aspects need to be considered to make it financially viable (Aiken et al., 2022, 2019). However, most pilot-scale MECs with anodic volumes of several litres report low hydrogen production rates of about 0.05 – 0.08 m^3 m^{-3} d^{-1} with poor current densities (< 1 A m^{-2}) (Rousseau et al., 2020). On the other hand, commercial electrolysers can reach hundreds or thousands of A m^{-2} but at the expense of high energy requirements (Rashid et al., 2015). While the development of pilot-scale water electrolysers has made notable strides, MECs remains a technology in need of further refinement to achieve widespread adoption.

One of the primary factors contributing to the limited performance of MECs at pilot-scale is the use of low organic strength urban wastewaters (0.25 – 0.80 g L^{-1}) (Tchobanoglous et al., 2014). In contrast, industrial wastewaters, generated by various manufacturing processes, exhibit distinct characteristics compared to urban wastewaters. They typically have a higher organic strength, ranging from strong (>1 g COD L^{-1}) to extremely strong (>200 g L^{-1}), as observed in olive mills (Paraskeva and Diamadopoulos, 2006), textile industries (Walker, 2001), and beverage production facilities (Valta et al., 2015). This high organic content makes industrial wastewater a potential feedstock for MECs, as it provides a rich source of electron donors for hydrogen production. Nonetheless, other physicochemical properties such as pH, salinity or toxicity, must be evaluated to ensure the suitability for MEC operation. The presence of inhibitory compounds or recalcitrant organic matter in industrial wastewaters may require pretreatment steps before being fed to MECs.

One of the current focuses of research when scaling-up MECs is to minimize ΔV losses to obtain a high hydrogen yield at a low energy input. Membrane-less MECs offer significantly lower resistance to current flow, but if metabolic inhibitors are not used, the gas produced contains impurities (such as methane, carbon dioxide or hydrogen sulphide) that require further post-treatment (Kadier et al., 2015). Additionally, hydrogen recycling to the anode, which has been documented in these systems and decreased the net hydrogen production, can also readily occur (Ruiz et al., 2013). Other researchers focus on minimising anodic mass transfer limitations by implementing a recirculation flow (Escapa et al., 2015; Zhang et al., 2010) or a flow-through anode (Rossi et al., 2020; Sleutels et al., 2009b). Similarly, the cathode overpotential can be reduced by decreasing mass transfer issues and improving the catalytic properties of the electrode to drive HER (Escapa et al., 2016). In this frame, Pt is one of the most common catalysts for electrochemical reactions, but its high-cost leads to increased and unaffordable capital expenses for MECs (Ambler and Logan, 2011). Therefore, increasing emphasis is being placed on the development of non-noble metal cathodes to ensure the economic viability of MECs.

Among the various cathodes with non-noble metals investigated for MECs, Ni-based cathodes have received significant attention (Kundu et al., 2013). Ni exhibits lower HER overpotential and greater stability at alkaline conditions compared to other common non-noble materials like stainless-steel (SS) (Chaurasia and Mondal, 2022; Lu et al., 2016). Also, Ni exhibits a significantly lower cost compared to Pt, and it is abundantly accessible on a large scale (it is a crucial material to produce SS and battery manufacturing) (Kadier et al., 2015). Ni and Ni alloys have been used as cathode in different formats, including as a metal sheet (Selembo et al., 2009), as a metal foam (Jayabalan et al., 2019; Jeremiasse et al., 2010), or as a powder (Kim and Logan, 2019; Selembo et al., 2010). In most of the lab tests, higher hydrogen production rates with Ni-based cathodes than other non-noble metal cathodes have been reported. However, its practical relevance on a larger scale is still unexplored. With this view, the main goal of this work was to test, for the first time at pilot-scale (>100 L), the use of Ni-foam as cathode material in a double-chamber cassette-type MEC treating industrial wastewater. The selection of Ni-foam was based on its high specific surface area, which leads to a lower activation overpotential compared to other Ni-based cathodes (Jeremiasse et al., 2010). The 150 L double-chamber MEC was operated in batch and continuous mode for over three months with real diluted industrial wastewater from a confectionery industry. The effect of Ni-foam in current generation and hydrogen production was studied and compared to a cassette operating with SS wool cathode (Baeza et al., 2017; Guerrero-Sodric et al., 2023). By exploring the limitations and challenges that arise when working on a larger scale, this research presents valuable insights into the practical feasibility and scalability of implementing Ni-foam as a cathode material in MECs treating wastewater.

2. Materials and methods

2.1. MEC pilot plant design

The pilot plant (Figures S1-S2) comprised seven cassette cells accommodated in a 220 L SS tank, each of which functioning as an independent double-chamber MEC. The cassettes were strategically positioned on alternating sides of the reactor with the intention to facilitate a zig-zag flow, as reported in our previous studies (Baeza et al., 2017; Guerrero-Sodric et al., 2023). The total anodic volume was 150 L after accommodating the cells. The cassettes were made of a PVC frame of 36 × 46 × 3 cm in the centre acting as a cathode chamber, and two outer PVC frames of 36 × 46 × 1 cm (with a 10 × 10 cm window) holding the anodes (Figures S3-S4). An anion exchange membrane (AEM) (RALEX® AMHPP, Mega, Czechia) was used to separate every anode and cathode. The selection of an AEM was made based on the lower transport resistance of ions through the membrane compared to cation exchange membranes (Sleutels et al., 2009a). Carbon felt (PX35 Carbon Felt, Zoltek™, United States) was used as anode. SS mesh was employed to tightly press the anode to the AEM. A 1 mm SS cross wire was wounded into the SS mesh for the electrical connections. To improve biomass adhesion, the carbon felt was pre-treated at 400 °C for 20 min. The projected anode surface of the reactor was 1.14 m^2, with 0.163 m^2 per each one of the seven cells. The overall reactor area-to-volume ratio was

7.6 m^2 m^{-3}.

Ni-foam (RCM-Ni4753, Recemat BV, The Netherlands) was used as cathode material to drive the HER. Ni-foam purity was 99.5 %, with surface density of 79 ± 3 g m^{-2}, porosity 95.2 %, with 0.4 mm pore diameter, and a specific surface of 5400 m^2 m^{-3}. The effect of Ni-foam in performance was studied under two cathode configurations (Fig. 1): i) Configuration NF_S (S stands for single), using a 15 × 20 cm sheet of Ni-foam placed in the centre of the cathodic chamber; ii) Configuration NF_D (D stands for double), with two 25 × 33 cm Ni-foam sheets attached to the membranes, which were electrically interconnected trough a titanium wire current collector. For this second configuration, polypropylene 3D-printed separators were used to fix the Ni-foam sheets in contact with the membranes while allowing catholyte flow inside the cathodic chamber (Figure S3-S5). The discrepancy in the Ni-foam sheet size between the single and double configurations (15 × 20 cm vs. 25 × 33 cm) was because a commercial sheet size was chosen to preliminarily assess the impact of Ni-foam on NF_S. After the good results obtained, the size of the Ni-foam sheet was increased up to the cathode chamber size to ensure sufficient active area in the NF_D.

Additionally, a cell (C5) with a SS cathode (Steel wool #2, Barlesa SL, Spain) (Baeza et al., 2017; Guerrero-Sodric et al., 2023) was operated for comparison purposes. Since only one SS cell was installed, the typical variability obtained in these previous works with the same type of cathode was used to estimate the possible variation of its current density. Table 1 shows the cathode configuration used in each cassette for each operational mode.

A gas collection port located on the top of the central frame facilitated the gas extraction through a tubing line (Marprene® Tubing 9.6 mm BORE, Watson Marlow, United Kingdom) linked to a gas sampling bag (V = 10 L, FlexFoil® Standard, SKC, United States). Additionally, 2.5 mm EPDM gaskets were employed between the frames to guarantee a robust and airtight seal.

2.2. MEC pilot plant operation

The cells were inoculated with anaerobic sludge from a nearby WWTP (Sabadell, Spain). A volume of 5 L of sludge was mixed with diluted wastewater and introduced in the anodic chamber. The volatile suspended solids (VSS) initial concentration in the anolyte was 1.5 g L^{-1}. The different modes of operation that were established in the pilot plant are detailed in Table 2. The reactor was started-up with six NF_S and one SS cells, in continuous mode at ΔV = 0.8 V, OLR = 1.00 g L^{-1} d^{-1} and HRT = 2 d. An anodic internal recycle flowrate of 200 L d^{-1} was maintained during the entire experimental trial. The catholyte in each cell was maintained without recirculation to avoid hydrogen losses. The influent flowrate and anodic internal recycle were established using two programmed peristaltic pumps (520 FAM/R2, Watson Marlow, United Kingdom). Wastewater was fed continuously during inoculation to reduce the solids retention time of the sludge, minimizing undesired precipitation and subsequent proliferation of biomass which could lead to undesired processes such as methanogenesis.

At day ~12, ΔV was increased from 0.8 V to 1.0 V, and the reactor was operated in discontinuous mode to investigate the impact of COD concentration on reactor performance. A total of four batches were performed using diluted wastewater. The initial COD concentration was 2 g L^{-1} in batches I/II and 5 g L^{-1} in batches III/IV. During this stage, the

Table 1
Cathode configuration employed in each cassette MEC.

Cell ID	Batch	Continuous
C1	NF_S	
C2	NF_S	
C3	NF_S	
C4	SS	
C5	NF_S	NF_D
C6	NF_S	NF_D
C7	NF_S	

Table 2
Details of the different operational stages of the MEC pilot plant.

Stage	Time (d)	Cell configuration	ΔV
Start-up	0 - 12	NF_S and SS	0.8
Batch mode	12 - 40	NF_S and SS	1
Continuous mode 1	45 - 70	NF_S, NF_D and SS	1
Continuous mode 2	70 - 97	NF_S, NF_D and SS	0.6 - 1.4

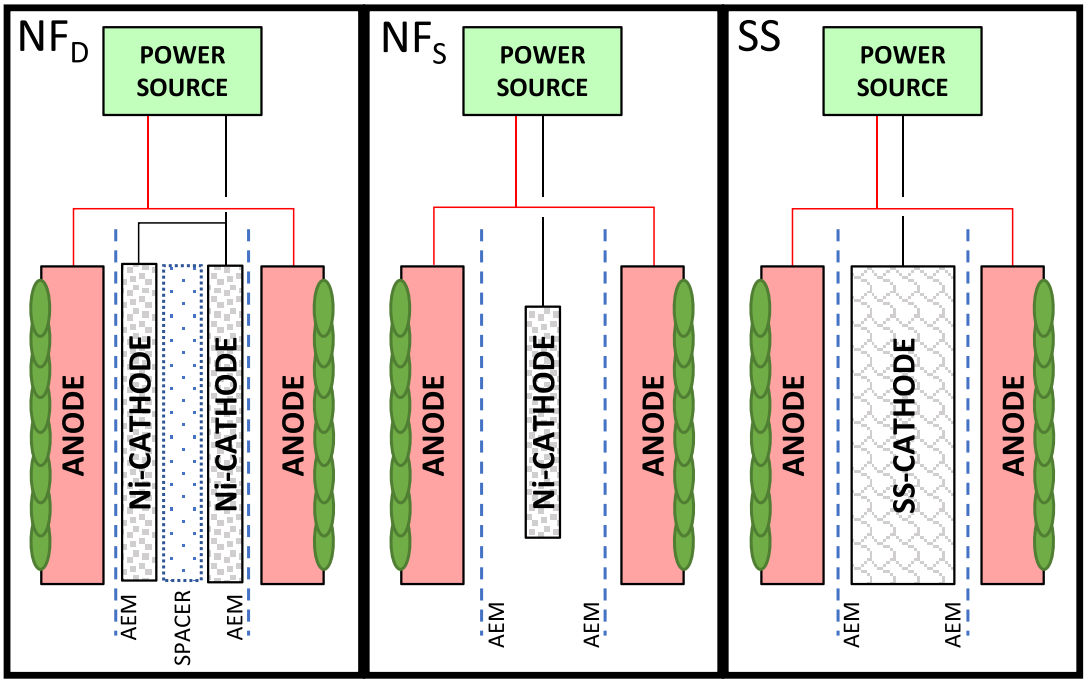

Fig. 1. Schematic representation of the cathode configurations tested.

pH in the anolyte was monitored but not controlled.

After the batch period, C4 and C5 were reassembled with the cathode configuration NF_D. Continuous operation with anodic pH control (20 g L^{-1} $NaHCO_3$ buffer solution addition, pH setpoint 7.0) was started in day 45 using diluted industrial wastewater with COD = 2 g L^{-1}, operating at HRT = 2.5 d, OLR = 0.82 g L^{-1} d^{-1} and ΔV = 1.0 V. Lastly, from day 70 onwards, the influence of the ΔV on the reactor performance was investigated. ΔV was incrementally raised from 0.60 V to 1.40 V in 0.10 V intervals, to cover a wide range of potentials. Hydrogen production was measured a minimum of three times at each ΔV tested.

2.3. Power supply and current monitoring

The applied voltage required for each cell was set by an independent programmable DC power source (Programmable DC LAB Power Supply 0 - 30 VDC USB LABPS3005DN, Velleman Goup, Belgium). The electrodes were connected to the power sources through 1.5 mm insulated copper wires. The AddControl software developed in NI LabWindows CVI (Baeza, 2022) was used to monitor current intensity and voltage in each cell at 5-minute intervals and recorded for the subsequent calculation of the key performance parameters.

2.4. Characteristics of wastewater

The real industrial wastewater was obtained from a sugar confectionery factory nearby Barcelona, Spain, and stored at 5 °C before use. The wastewater had a turbid appearance, pale orange colour and sweet odour. The wastewater contained 22.1 g L^{-1} saccharose, 18.4 g L^{-1} glucose, 16.2 g L^{-1} fructose, 8.6 g L^{-1} lactose, 4.3 g L^{-1} maltose, and contained proteins and fats. Diluted industrial wastewater was used as substrate for the microbial community in the anode chamber. All dilutions were prepared with demineralized water with no extra addition of buffer solution or nutrients. The important physicochemical properties of the raw wastewater and the dilutions are listed in Table 3.

2.5. Analytical methods

Liquid samples from the anode chamber were characterized after filtering effluent samples with 0.22 μm pore filters. The quantification of organic matter was conducted using commercially available COD kits (Hach, LCK 514, United States), capable of measuring within a range of 0.1 – 2 g O_2 L^{-1}. The readings were performed using a spectrophotometer (Hach, DR2800). Total N was analysed by a combustion device at high temperature (Multi N/C® 2100S, Analytik Jena, Germany). Phosphate was measured with a PHOSPHAXsc analyser using the vanadomolybdate yellow method (Hach Lange). Gas chromatography (Agilent Technologies, 7820-A) was used to measure ethanol and volatile fatty acids (VFA), including acetic, propionic, isobutyric, butyric, isovaleric, valeric, isocaproic and caproic acids. The detector was based on flame ionization and the column was a DB FFAP (30 m x 0.25 mm x 0.25 μm). 800 μL of filtered anolyte were transferred to a chromatography vial to which 200 μL of a stabilizing solution composed of crotonic acid (2 g L^{-1}) and phosphoric acid (2 %) was subsequently added. The pH in the anode was continuously monitored (HACH pH electrode Crison5233, Spain), while conductivity was measured offline with a conductivity meter (XS Instruments COND 8, Italy).

The cathodic gas was analysed by gas chromatography (Agilent Technologies, 7820-A). Two columns were used: i) Porapaq Q 80/100 3 ft G3591–81,136 (1.38 *m* ± 2 mm) and ii) MolSieve 5 A 80/100 3 ft. G3591–80,017 (1.83 *m* ± 2 mm). Hydrogen and methane production was determined through the Gas Bag Method (Ambler and Logan, 2011). A detailed description is available in the supplementary information.

2.6. Molecular methods

The microbial community composition was determined by 16S rRNA gene Illumina amplicon sequencing. During the decommissioning process at the conclusion of the experimental trial, samples of anodes were collected. The DNA extraction process was performed using a Soil DNA isolation plus kit (Norgen Biotek CORP, Canada). The carbon felt was cut into small pieces using a sterilized scalpel and added to the lysing matrix tube. Each tube held wet carbon felt with a weight of 10.00 *g* ± 0.02 g. The cell lysis, DNA isolation, and purification procedures were carried out in accordance with the instructions of the manufacturer. The concentration and the quality of the DNA extracted were analysed with a spectrophotometer (NanoDrop 1000,Thermo Fischer Scientific, USA). A 260/280 ratio of 1.8 ± 0.1 was selected as a good quality indicator and a DNA concentration of 5 ng μL^{-1} was required as the minimum concentration needed for sequencing. Prior to further analyses, DNA samples were stored at −20 °C. Sequencing analyses were carried out by the Genomics Service (SG) of the Universitat Autònoma de Barcelona (UAB, Spain). The organisms were categorized using the RefSeq+RDP database (Alishum, 2022) and the sequence reads were examined using Usearch software. Each anode sample was extracted and sequenced twice, one for each carbon felt of the same cassette, so the results presented in this work correspond to the average of two sequencing analyses.

2.7. Key performance indicators (KPIs)

Current density (*j*) was calculated by normalizing the electrical current by the projected anodic surface area (A m^{-2}). The hydrogen produced was quantified based on the volumetric production rate per unit anodic surface area (L m^{-2} d^{-1}) or reactor volume (m^3 m^{-3} d^{-1}). Cathodic gas recovery efficiency (r_{CAT}) was calculated by comparing the number of electrons necessary for hydrogen production to the number of electrons reaching the cathode as electrical current. Coulombic efficiency (CE) was determined by comparing the coulombs recovered as current to the theoretical coulombs generated from substrate oxidation. Energy production (E_P, kWh d^{-1}) was calculated as the amount of energy recovered in the form of hydrogen. Energy consumption (E_C, kWh d^{-1}) was determined as the amount of electrical energy produced by the power sources. Energy recovery (r_E) was evaluated as the ratio of energy production to energy consumption, providing an indication of the overall energy efficiency of the MEC system. The calculations for the KPIs were performed as described previously (Guerrero-Sodric et al., 2023), and can be found in the supplementary information.

3. Results and discussion

3.1. Pilot plant start-up

The reactor was inoculated using anaerobic sludge and started-up in continuous mode at ΔV = 0.8 V, OLR = 1.00 g L^{-1} d^{-1}, and HRT = 2 d with an internal recycle of 200 L d^{-1} (1.3 refills of the anodic volume

Table 3
Physicochemical properties of the raw and diluted industrial wastewater.

Wastewater	COD_S (g L^{-1})	Total N (mg L^{-1})	$P\text{-}PO_4^{3-}$ (mg L^{-1})	Conductivity (mS cm^{-1})	pH
Raw IWW	74 ± 2	642 ± 37	26 ± 1	1.4 ± 0.1	7.1 ± 0.1
Diluted IWW	2.04 ± 0.02	8 ± 1	1 ± 1	0.3 ± 0.1	6.8 ± 0.1
	5.01 ± 0.02	18 ± 2	2 ± 1	0.6 ± 0.1	6.5 ± 0.1

per day). All cassettes showed similar exponential intensity profiles during inoculation, with a lag phase of ~3.5 d and reaching a stable current after approximately 10 d of operation (Figure S6). Despite the six NFs cassettes were assembled and started-up identically, some variability was observed among the cells regarding their current density and hydrogen production. The maximum intensity in the NF_S cells during inoculation ranged from 0.118 A to 0.152 A, the average current density was 0.82 ± 0.09 A m^{-2}, and the specific H_2 production rate was 7.29 ± 1.57 L H_2 m^{-2} d^{-1}. Inoculation was considered to be finished at day ≈ 12 (t = 11.89 d) when stable performance over time was observed in all cells.

3.2. Preliminary evaluation of the performance of Ni-foam

Several batch tests were performed with the objective of gaining initial insights into the material's behaviour and understanding the influence of concentration on the plant performance. In batches I/II (ΔV = 1.0 V; initial COD = 2 g L^{-1}), current density and hydrogen production showed a close relation with the COD concentration in the anolyte (Fig. 2). Current density peaked two days after the substrate was loaded and gradually dropped at COD concentrations below ≈1 g L^{-1} (Fig. 2B). The profiles obtained are consistent with the proposed synergistic mechanisms for the oxidation of complex substrates in bioelectrochemical systems (Montpart et al., 2015). Sugars, proteins, and fats in the wastewater need to be hydrolyzed and fermented to VFA in order to be used by the exoelectrogenic community. Hence, when complex organics were fed, there was a first stage in the batch when ARB were limited by low VFA presence. As the complex organic compounds were fermented, VFA production increased and, therefore, the anodic biofilm activity. Then, current density declined when substrate was depleted.

At high COD concentrations (> 1 g L^{-1}), NF_S cells reached a maximum average current density of 1.01 ± 0.02 A m^{-2} and H_2 production of 8.87 ± 1.15 L m^{-2} d^{-1}, which was a 1.1-fold and 1.2-fold higher, respectively, than those values obtained in the SS cell (0.89 A m^{-2} and 7.41 L H_2 m^{-2} d^{-1}). In contrast, NF_S and SS cells exhibited similar performance at low COD concentrations (< 1 g L^{-1}), with less than 5 % of difference between both cathode materials under such conditions. For instance, the current density observed with both cathode materials was around 0.73 A m^{-2} at the end of batch I (t = 16.37 d; COD ≈ 0.70 g L^{-1}), and 0.30 A m^{-2} at the end of batch II (t = 23.43 d; COD ≈ 0.25 g L^{-1}). This behaviour could be attributed to the low COD concentration limiting the anodic biofilm activity. This is an important fact to consider in future MEC designs: anode performance is likely to be the limiting factor in low-strength wastewater treatment applications. Then, the use of expensive cathode materials to enhance HER may not be cost-effective, as the activation and concentration overpotentials in the anode would be the dominant limiting factor.

During batches III/IV, there was no significant enhancement in performance despite increasing the initial COD concentration up to 5 g L^{-1}. Current density peaks were similar to those recorded in batches I/II but more sustained over time, with NFs cells yielding between 30 - 40 %

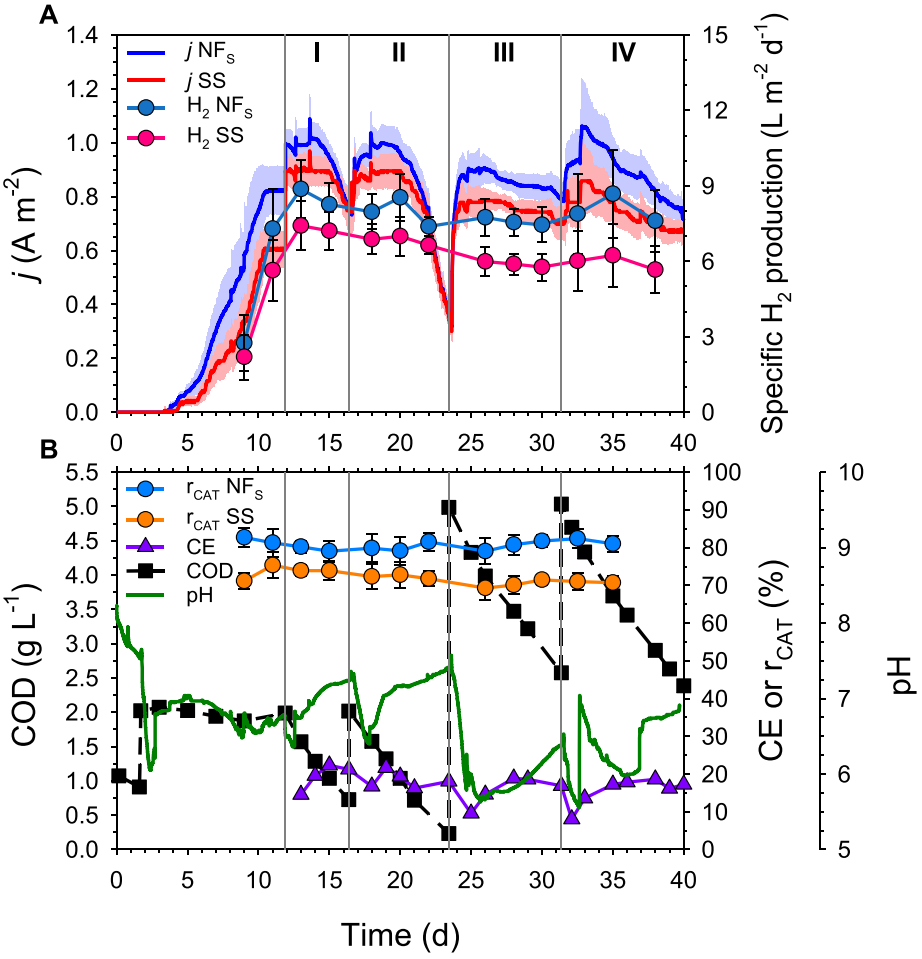

Fig. 2. Start-up and batch operation profiles. A) Average current densities (j) and specific hydrogen production rates of the single-sheet nickel-foam cells (NF_S) and the stainless-steel cell (SS). B) Anodic COD concentration, pH and coulombic efficiency (CE); Average cathodic recovery efficiencies (rCAT) of the NF_S and SS cells. Shade indicates standard deviation of current density in the NF_S cells (experimental) and SS cell (estimated as described in Section 2.1). The grey dashed line indicates the start of a new batch.

Table 4
Summary of the most important results obtained during the batch tests.

					NF_S (C1 - 3, 5 - 7)		SS (C4)	
Batch ID	Batch length (d)	ΔCOD (mg L^{-1})	CE (%)	pH	j_{max} (A m^{-2})	H_{2max} (L m^{-2} d^{-1})	j_{max} (A m^{-2})	H_{2max} (L m^{-2} d^{-1})
I	4.5	1262	19	6.95 ± 0.26	1.02 ± 0.02	8.87 ± 1.15	0.89	7.42
II	7.1	1784	18	7.08 ± 0.26	1.01 ± 0.07	8.54 ± 0.94	0.90	6.99
III	7.9	2409	15	6.08 ± 0.45	0.91 ± 0.06	7.75 ± 0.75	0.79	5.98
IV	8.6	2647	16	6.37 ± 0.37	1.06 ± 0.12	8.68 ± 1.75	0.85	6.24

j_{max}: Maximum current density; H_{2max}: Maximum specific hydrogen production rate; pH: Average pH; ΔCOD: COD concentration difference between the start and the end of the batch; CE: Coulombic efficiency.

higher specific hydrogen production rate than the SS cell (Table 4). NFs cells achieved slightly higher cathodic recovery efficiencies (r_{CAT}) among the different batches (81 ± 1 % for NFs vs 73 ± 2 % for SS, Fig. 2). These are promising results considering that the cathodic efficiencies reported at pilot-scale are usually below 60 % (Jiang et al., 2023). This achievement underscores the efficacy of our double-chamber configuration in efficiently capturing the hydrogen generated at the cathode.

Despite achieving significant COD degradation (Table 4), CEs lower than 20 % (17 ± 2 %) were observed, indicating that considerable biological organic matter oxidation other than exoelectrogenesis was occurring. These alternative pathways likely involved heterotrophic oxidation in the upper reactor layers and methanogenesis in the lower anaerobic regions. Thus, the organic removal rates observed were not significantly dependent on hydrogen production or current generation. This scenario is frequently observed in pilot-scale double-chamber MECs and is linked to the elevated biological activity of planktonic biomass present in the anode chamber (Guisasola et al., 2020).

As shown in Fig. 2 and detailed in Table 4, batches III/IV reached lower pH levels compared to batches I/II as the higher initial COD concentration led to the accumulation of fermentation products. The impact of pH was evident at day ≈ 32 (t = 32.40 days), when the pH of the anolyte was risen from 5.6 to a neutral value, boosting current density and hydrogen production. However, the COD concentration was still high, and the reactor was again acidified by fermentation. These differences in pH had considerable implications on the microbial community composition within the bioreactor. Therefore, the lack of improvement compared to batches I/II was mainly attributed to significant anolyte acidification (pH < 6), which masked any potential effects of the increased COD on current generation. For this reason, a pH control was implemented from day 37 (t = 36.88 d) onwards to maintain a neutral pH in the anolyte for the next experiments.

3.3. Performance and cost analysis of the different cathode configurations

Following the 40 days of batch operation, C4 and C5 were reassembled with a new bi-cathode configuration using two 30 × 35 cm interconnected Ni-foam sheets attached to the membranes (NF_D in Fig. 1). The continuous operation with anodic pH control (pH = 7) was started in day 45 using diluted industrial wastewater with an inlet COD concentration around 2 g L^{-1}, operating at ΔV = 1.0 V; HRT = 2.5 d; and OLR = 0.82 g L^{-1} (Fig. 3). The ORR remained around 0.33 ± 0.02 g L^{-1} d^{-1} during the whole continuous operation and the chemical composition of the effluent was 0.40 ± 0.01 g L^{-1} acetic acid, 0.11 ± 0.00 g L^{-1} propionic acid, 0.10 ± 0.00 g L^{-1} ethanol, and 0.05 ± 0.00 g L^{-1} butyric acid. These compounds represented ≈95 % of the total COD in the effluent, suggesting that the organic macromolecules in the influent were effectively transformed into fermentation products. The measured CE was generally low as reported in batch mode (CE = 21 ± 2%), indicating room for improvement in terms of energy efficiency in future MEC designs (Figure S7). Furthermore, there were no substantial differences in the r_{CAT}, being the NF_D cells those with the highest value: 86 ± 2%.

The start-up of the two NF_D cells led to different current densities and hydrogen production rates but reached similar values (around 1.85 A m^{-2} and 17.86 ± 0.89 L H_2 m^{-2} d^{-1}) from day ≈ 62 onwards (Fig. 3 and S8). The average rate of hydrogen production observed in the NF_D configuration was 3.0-fold higher than that obtained with the SS cell and 1.8-fold higher than the NF_S cells. This enhancement in performance was attributed to the higher cathode surface and lower electrode spacing, which resulted in a reduction of the overall ohmic resistance and a more efficient energy utilisation.

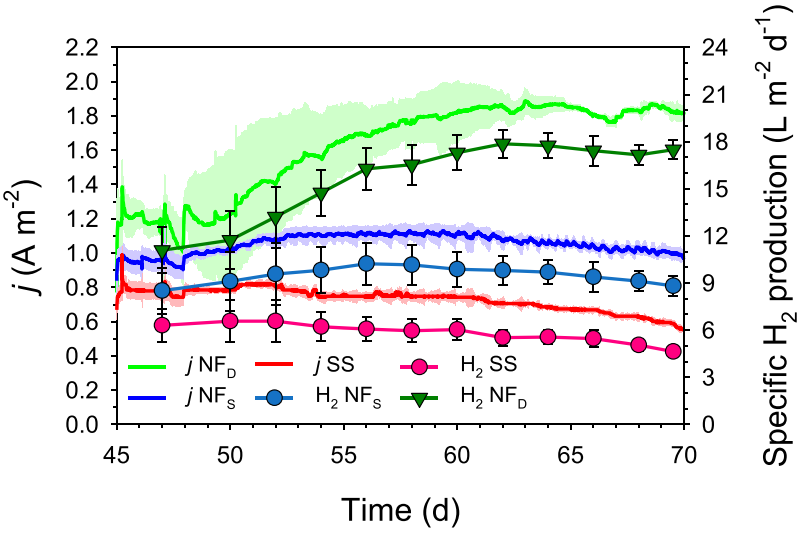

Fig. 3. Average current density (j) and specific hydrogen production over time in each configuration for the continuous operation using diluted industrial wastewater.

Despite the NF_D cells exhibited a higher current density in comparison to the NF_S cells, their current density normalized to the projected cathodic surface was three times lower than that of the NF_S cells (1.79 A m^{-2} and 5.32 A m^{-2} for the NF_D and NF_S cells, respectively). These findings suggest that the cathode in NF_D cells was oversized and, hence, the cathode surface could probably be optimised to improve the specific performance of the MEC. Furthermore, the NF_D configuration was more expensive due to the higher price of Ni-foam compared to SS wool (540 € kg^{-1} vs. 10 € kg^{-1}). The amount of cathode employed was 0.04 kg and 0.22 kg of Ni-foam for the NF_S and NF_D configurations, respectively, and 0.38 kg of SS wool for the SS cell. Therefore, the cathode cost of a cassette was 22 €, 119 € and 4 € for the NF_S, NF_D and SS configurations, respectively. This is a 5.5-fold and 29.8-fold increase in the cathode cost compared to the SS wool configuration, which is not corresponded by the cell performance regarding current density and/or hydrogen production. However, the selection of the optimal cathode material depends on the specific system requirements or potential budget constraints. Additionally, factors such as the longevity of the cathode material, or its potential reusability, should be further studied, as these factors could significantly impact the economic feasibility of the technology,

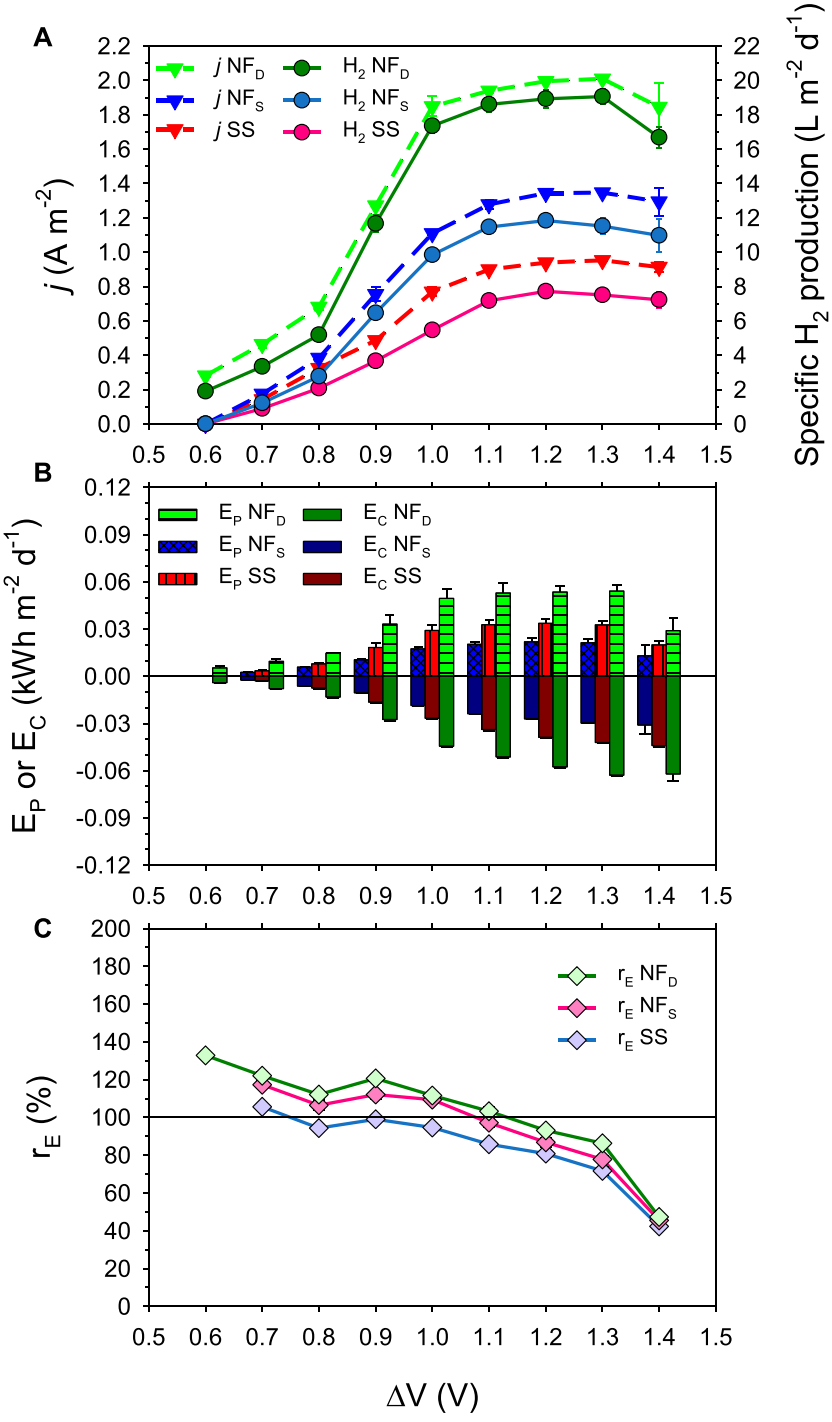

Fig. 4. Key performance indicators of the double-sheet nickel-foam cassettes (NF_D), single-sheet nickel-foam cassettes (NF_S) and the stainless-steel cassette (SS), at different applied potentials (ΔV) for continuous operation. A) Average current density (*j*) and specific hydrogen production rate. B) Average energy production (E_P) and energy consumption (E_C). C) Energy recovery efficiency (r_E).

particularly when considering large-scale implementation. Furthermore, the additional cost of the membrane to maintain the required two-chamber configuration should also be considered. Throughout the operation in this work, no clogging or deterioration was observed, but the long-term stability of the membrane should be studied to obtain a good estimation of the associated cost.

3.4. Effect of ΔV on production of hydrogen and energy efficiency

At day 70, different ΔVs were tested maintaining the same hydraulic conditions and temperature to investigate the influence of the energy applied on the reactor performance. ΔV was increased from 0.60 V to 1.40 V, in 0.10 V intervals (Fig. 4). After a short non-steady state period, stable current density and hydrogen production over time was observed in all cells for every ΔV tested (Figure S9). The only exception was at an ΔV of 1.4 V when the performance declined in all configurations, indicating the occurrence of side reactions or electrode degradation processes that adversely affected the bioelectrochemical behaviour of the cells. NF_D cells showed the lowest potential loss of all configurations tested, exhibiting a minimum ΔV requirement of 0.60 V to produce hydrogen (1.90 ± 0.14 L H_2 m^{-2} d^{-1}) (Fig. 4A), with a current density of 0.28 ± 0.00 A m^{-2}. In contrast, SS and NF_S cassettes required a higher minimum ΔV of 0.70 V and generated around 1 L H_2 m^{-2} d^{-1} with a current density of 0.14 A m^{-2}. Notably, NF_D and NF_S cells exhibited a sigmoidal trend, with a maximum average hydrogen production of 19.07 ± 0.46 L H_2 m^{-2} d^{-1} and 11.85 ± 0.40 L H_2 m^{-2} d^{-1}, respectively. On the other hand, SS cell displayed a more gradual increase in hydrogen production with the ΔV, eventually reaching a maximum of 7.72 ± 0.39 L H_2 m^{-2} d^{-1} at ΔV = 1.2 V. The initial region of the sigmoidal curve (low ΔV) indicates limitations of ΔV whereas the last region indicates mass transfer limitations, since the current density does not depend on the ΔV.

The hydrogen production rates under different ΔVs resulted in different energy recovery efficiencies (r_E) of the system (Fig. 4C). Regardless of the cathode configuration, a higher ΔV within the cells correlated with reduced r_E. The highest energy recovery efficiency ($r_E = 132 \pm 1\%$) was obtained in the NF_D cells at the minimum applied potential (ΔV = 0.60 V). The optimal ΔV (i.e. balancing energy input/output) for all configurations was found to be in the range 0.9 – 1.0 V, in which a reasonable hydrogen production can be reached without compromising the energy efficiency of the process. NF_D and NF_S cells not only achieved energy neutrality but were net energy producers in a wide range of ΔV, since the hydrogen would yield up to 0.05 kWh m^{-2} and 0.01 kWh m^{-2}, respectively. In contrast, the SS cell exhibited higher energy requirements with lower energy production yields for all investigated ΔV, but could reach energy neutrality in some cases (e.g. ΔV = 0.7/0.9 V).

Assuming full-operation of the pilot plant with 10 NF_D cells in the bioreactor ($S / V = 12.6$ m^2 m^{-3}), this configuration could potentially generate up to 0.21 m^3 H_2 m^{-3} d^{-1} with r_E >100%. This is a significant outcome of this work since the reported H_2 production rates in double-chamber MEC pilot (>100 L) are usually in the range of 0.005 – 0.040 m^3 m^{-3} d^{-1} (Guisasola et al., 2020). The benefits of using Ni-based cathode materials have already been reported at lab-scale and compared to Pt sheets (Hu et al., 2009; Selembo et al., 2009), enabling theoretical volumetric hydrogen production rates as high as 50 m^3 H_2 m^{-3} d^{-1} (Jeremiasse et al., 2010). However, scaling-up and obtaining similar performance to lab-scale set-ups is the current bottleneck of bioelectrochemical systems. Scaling-up at volumes >100 L entails additional complexities and challenges, including mass transport limitations and reactor design considerations. Therefore, while lab-scale experiments provide valuable insights, further investigation and validation at pilot scale are necessary to determine the true potential and performance of new cathode materials in practical applications.

3.5. Bacterial communities in the anode

Samples from the anodes of the NF_D and SS cassettes were analysed by Illumina 16 s. The analysis of the microbial community revealed that the cathode material significantly influenced the composition of the biofilm. A more efficient cathode results in lower cathode overpotential and, thus, varies the anode potential. It is well established that different anode potentials may lead to slightly different microbial communities. The microbial community developed on the anode of both types of cassettes was a mixed consortium with similar dominant orders but with different relative abundances. For instance, in the NF_D samples, the dominant orders were *Desulfuromonadales* (26.8 %), *Bacteroidales* (24.9 %), *Enterobacteriales* (15.1 %), *Desulfovibrionales* (8.5 %) and *Clostridiales* (4.5 %). For the SS sample, the relative abundance was *Desulfuromonadales* (15.8 %), *Bacteroidales* (12.9 %), *Enterobacteriales* (15.1 %), *Clostridiales* (7.5 %) and *Desulfovibrionales* (7.1 %).

The dominant genus in the NF_D cells were *Geobacter* (16.9 %) and *Bacteroides* (15.4 %) (Fig. 5). *Geobacter* species are known as efficient exoelectrogens, capable of harvesting electrical energy from organic compounds (Kumar et al., 2015; Logan and Regan, 2006). On the other hand, *Bacteroides* species are known to be able to hydrolyse proteins and carbohydrates (Mahadevan et al., 1980). As suggested in other studies about MECs, they could have the role of hydrolysis and fermentation of complex organics into VFA (Wang et al., 2010). Previous works have already demonstrated the need to develop an anodic biofilm with a syntrophic consortium between fermentative bacteria and exoelectrogens to treat complex substrates with bioelectrochemical systems (Montpart et al., 2015). Other dominant genera were *Desulfovibrio* (8.5 %) and *Klebsiella* (7.0 %). *Desulfovibrio* species are sulphate-reducing bacteria (Postgate and Campbell, 1966) that can participate in syntrophic relationships with exoelectrogens, facilitating the removal of sulphate and promoting the overall performance of the MEC. *Klebsiella* is a genus of facultative anaerobic bacteria that can carry out different metabolic processes, including fermentation and nitrogen fixation (Drancourt et al., 2001; Rosenblueth et al., 2004).

The results at genus level clearly show an important fraction of unclassified and other microorganisms, which implies a high diversity because of working with a complex industrial wastewater. Comparing the results of NF_D with those of SS, the proportion of *Geobacter* is reduced to 8.1 % in the latter, which is clearly correlated with the lower exoelectrogenic activity observed. A lower proportion of *Bacteroides* is also observed (6.6 % for SS), which implies a higher proportion of other microorganisms and corroborates the hypothesis that biofilms developed using NF_D as cathode have higher specificity and seem to be more suitable for generating exoelectrogenic activity. The Shannon Diversity index at the genus level further supports this statement, with values of 3.06 and 3.72 for the NF_D and SS configurations, respectively, indicating a higher level of microbial diversity in the SS biofilm.

The 16S rRNA clone libraries revealed that three *Geobacter* strains collectively constitute 15.4 % of the NF_D community: *Geobacter chapellei* (7.8 %), *Geobacter pickeringii* (6.3 %) and *Geobacter sulfurreducens* (1.3 %). *Bacteroides_oleiciplenus*, a fermentative gram-negative bacterium belonging to the *Bacteroides* genus, comprised ≈15 % of the anodic communities. The major end products of glucose metabolism are acetic, succinic, formic and lactic acids (Watanabe et al., 2010).

Due to the limitations of the sampling method, microbial data could only be collected at the end of the experimental period, which restricted the scope of analysis regarding the influence of microbial composition on performance. However, the microbial consortium in both configurations appears to be well-suited for the transformation of organic macromolecules into energy. *Geobacter* species contribute significantly to the exoelectrogenic activity, while *Bacteroides* and other fermentative bacteria are involved in the production of VFA from sugar metabolism. These VFA can then be consumed by exoelectrogens, completing the energy conversion process in the MEC. The higher prevalence of exoelectrogenic microorganisms, along with the presence of fermentative

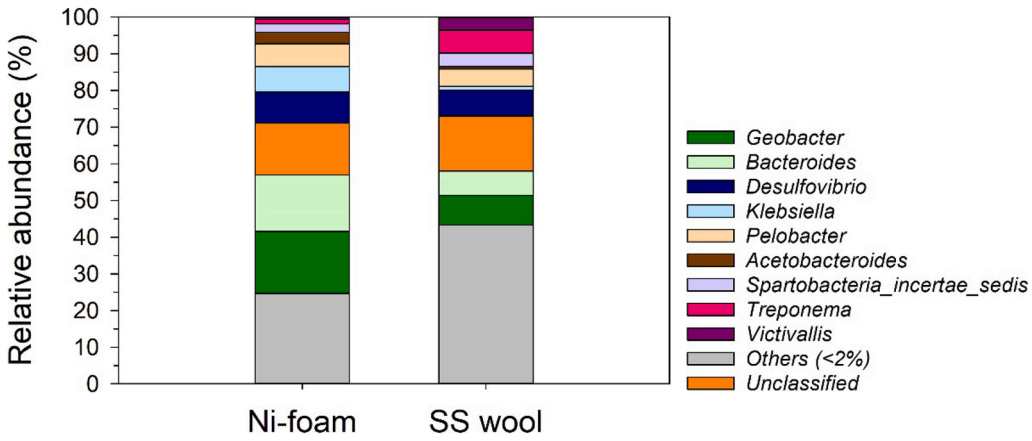

Fig. 5. Anodic bacterial communities at genus level based on cloned 16S rRNA gene sequence distribution for the double-sheet nickel foam (NF_D) and stainless-steel (SS) cassettes after reactor decommissioning.

bacteria, creates a more favourable environment for electron transfer and organic matter degradation in the NF_D cassettes, resulting in improved performance.

In the symbiotic relationship between exoelectrogenic and fermentative bacteria in the biofilm, ARB are likely to grow in the inner layers, closer to the conductive material, to efficiently donate the electrons generated in the anaerobic oxidation. In contrast, fermentative bacteria are likely to occupy the outer layers, providing a metabolic advantage by readily accessing fermentable substrates. These fermentative bacteria metabolize these substrates, generating acetate as a primary byproduct. Acetate, being a diffusible molecule, permeates the biofilm, reaching the exoelectrogenic population in the inner layers. If acetate availability is sufficient, ARB consume it, fuelling their growth and electron uptake. However, mass transfer limitations within the biofilm can restrict acetate diffusion, potentially limiting ARB growth. Fermentative bacteria, unaffected by fermentable substrate limitations, continue to produce and release acetate into the surroundings, contributing to the overall metabolic exchange within the biofilm. It is important to note that there may be other planktonic microorganisms in the anodic chamber that also produce and consume acetate.

4. Conclusions

This work is the first experimental demonstration that a MEC pilot plant (>100 L) can be successfully run with real industrial wastewater from the confectionery industry with i) good hydrogen production results (19.07 L m^{-2} d^{-1} and 0.21 m^3 m^{-3} d^{-1}), ii) reasonably high current density (2 A m^{-2}) and iii) considerable organic matter removal efficiency (40%).

High COD concentration allows high current densities, but the CE (around 20%) shows that other simultaneous organic matter removal processes occur, possibly related to heterotrophic oxidation in the upper layers of the reactor and methanogenesis in the lower part due to anaerobic conditions.

This work shows for the first time a novel cassette configuration with a double Ni-foam sheet cathode that offers the best current density and hydrogen production rates observed so far at this scale. The improvement with the novel configuration is 202 % over the SS-wool cathode and by 81 % over the configuration with only a single nickel foam sheet.

The applied potential has two opposite consequences regarding the energy efficiency of the system: on the one hand, higher ΔV imply higher energy requirements but also higher hydrogen (and thus, energy) recovery. A conservative value of 0.9 - 1.0 V was found to be successful for our system.

The anodic microbial community is a syntrophic culture of exoelectrogens and fermenters (mostly *Geobacter* and *Bacteroides*), which correlates well with the observed exoelectrogenic activity.

CRediT authorship contribution statement

Oscar Guerrero-Sodric: Writing – original draft, Visualization, Project administration, Methodology, Investigation, Formal analysis, Data curation, Conceptualization. **Juan Antonio Baeza:** Writing – review & editing, Visualization, Validation, Supervision, Software, Resources, Methodology, Investigation, Formal analysis, Conceptualization. **Albert Guisasola:** Writing – review & editing, Supervision, Resources, Project administration, Methodology, Investigation, Funding acquisition, Formal analysis, Conceptualization.

Declaration of competing interest

The authors declare that they have no known competing financial interests or personal relationships that could have appeared to influence the work reported in this paper.

Data availability

Data will be made available on request.

Acknowledgements

This work was supported by the LIFE+ NIMBUS project (LIFE19 ENV/ES/000191) (www.life-nimbus.eu). The authors are members of the GENOCOV research group (Grup de Recerca Consolidat de la Generalitat de Catalunya, 2021 SGR 515, www.genocov.com).

Supplementary materials

Supplementary material associated with this article can be found, in the online version, at doi:10.1016/j.watres.2024.121616.

References

Aiken, D.C., Curtis, T.P., Heidrich, E.S., 2022. The rational design of a financially viable microbial electrolysis cell for domestic wastewater treatment. Front. Chem. Eng. 3, 1–15. https://doi.org/10.3389/fceng.2021.796805.

Aiken, D.C., Curtis, T.P., Heidrich, E.S., 2019. Avenues to the financial viability of microbial electrolysis cells [MEC] for domestic wastewater treatment and hydrogen production. Int J Hydrogen Energy 44, 2426–2434. https://doi.org/10.1016/j.ijhydene.2018.12.029.

Alishum, A., 2022. DADA2 formatted 16S rRNA gene sequences for both bacteria & archaea. https://doi.org/10.5281/ZENODO.6655692.

Ambler, J.R., Logan, B.E., 2011. Evaluation of stainless steel cathodes and a bicarbonate buffer for hydrogen production in microbial electrolysis cells using a new method for

measuring gas production. Int. J. Hydrogen. Energy 36, 160–166. https://doi.org/10.1016/j.ijhydene.2010.09.044.
Baeza, J.A., 2022. Advanced Direct Digital Control (AddControl): lessons learned from 20 years of adding control to lab and pilot scale treatment systems. In: 13th IWA Conference on Instrumentation. Control and Automation. ICA 2022. Tsinghua University, Beijing (China), pp. 13–15.
Baeza, J.A., Martínez-Miró, À., Guerrero, J., Ruiz, Y., Guisasola, A., 2017. Bioelectrochemical hydrogen production from urban wastewater on a pilot scale. J. Power. Sources. 356, 500–509. https://doi.org/10.1016/j.jpowsour.2017.02.087.
Carmo, M., Fritz, D.L., Mergel, J., Stolten, D., 2013. A comprehensive review on PEM water electrolysis. Int. J. Hydrogen. Energy. https://doi.org/10.1016/j.ijhydene.2013.01.151.
Chaurasia, A.K., Mondal, P., 2022. Enhancing biohydrogen production from sugar industry wastewater using Ni, Ni–Co and Ni–Co–P electrodeposits as cathodes in microbial electrolysis cells. Chemosphere 286. https://doi.org/10.1016/j.chemosphere.2021.131728.
Drancourt, M., Bollet, C., Carta, A., Rousselier, P., 2001. Phylogenetic analyses of Klebsiella species delineate Klebsiella and Raoultella gen. nov., with description of Raoultella ornithinolytica comb. nov., Raoultella terrigena comb. nov. and Raoultella planticola comb. nov. Int. J. Syst. Evol. Microbiol. 51, 925–932. https://doi.org/10.1099/00207713-51-3-925/CITE/REFWORKS.
El-Emam, R.S., Özcan, H., 2019. Comprehensive review on the techno-economics of sustainable large-scale clean hydrogen production. J. Clean. Prod. https://doi.org/10.1016/j.jclepro.2019.01.309.
Escapa, A., Mateos, R., Martínez, E.J., Blanes, J., 2016. Microbial electrolysis cells: an emerging technology for wastewater treatment and energy recovery. from laboratory to pilot plant and beyond. Renew. Sustain. Energy Rev. https://doi.org/10.1016/j.rser.2015.11.029.
Escapa, A., San-Martín, M.I., Mateos, R., Morán, A., 2015. Scaling-up of membraneless microbial electrolysis cells (MECs) for domestic wastewater treatment: bottlenecks and limitations. Bioresour. Technol. 180, 72–78. https://doi.org/10.1016/j.biortech.2014.12.096.
Guerrero-Sodric, O., Baeza, J.A., Guisasola, A., 2023. Exploring key operational factors for improving hydrogen production in a pilot-scale microbial electrolysis cell treating urban wastewater. Chem. Eng. J. 469 https://doi.org/10.1016/j.cej.2023.144001.
Guisasola, A., Baeza, J.A., Marone, A., Trably, É., Bernet, N., 2020. Opportunities for hydrogen production from urban/industrial wastewater in bioelectrochemical systems. Microbial Electrochemical Technologies. CRC Press, Boca Raton, pp. 225–243. https://doi.org/10.1201/9780429487118-15.
Guo, Z., Sun, Y., Pan, S.Y., Chiang, P.C., 2019. Integration of green energy and advanced energy-efficient technologies for municipal wastewater treatment plants. Int. J. Environ. Res. Public Health. https://doi.org/10.3390/ijerph16071282.
Hu, H., Fan, Y., Liu, H., 2009. Hydrogen production in single-chamber tubular microbial electrolysis cells using non-precious-metal catalysts. Int. J. Hydrogen. Energy 34, 8535–8542. https://doi.org/10.1016/j.ijhydene.2009.08.011.
Jayabalan, T., Matheswaran, M., Naina Mohammed, S., 2019. Biohydrogen production from sugar industry effluents using nickel based electrode materials in microbial electrolysis cell. Int. J. Hydrogen. Energy 17381–17388. https://doi.org/10.1016/j.ijhydene.2018.09.219.
Jeremiasse, A.W., Hamelers, H.V.M., Saakes, M., Buisman, C.J.N., 2010. Ni foam cathode enables high volumetric H2 production in a microbial electrolysis cell. Int. J. Hydrogen. Energy 35, 12716–12723. https://doi.org/10.1016/j.ijhydene.2010.08.131.
Jiang, J., Lopez-Ruiz, J.A., Bian, Y., Sun, D., Yan, Y., Chen, X., Zhu, J., May, H.D., Ren, Z. J., 2023. Scale-up and techno-economic analysis of microbial electrolysis cells for hydrogen production from wastewater. Water. Res. 241, 120139 https://doi.org/10.1016/j.watres.2023.120139.
Kadier, A., Simayi, Y., Chandrasekhar, K., Ismail, M., Kalil, M.S., 2015. Hydrogen gas production with an electroformed Ni mesh cathode catalysts in a single-chamber microbial electrolysis cell (MEC). Int. J. Hydrogen. Energy 40, 14095–14103. https://doi.org/10.1016/j.ijhydene.2015.08.095.
Kim, K.Y., Logan, B.E., 2019. Nickel powder blended activated carbon cathodes for hydrogen production in microbial electrolysis cells. Int. J. Hydrogen. Energy 44, 13169–13174. https://doi.org/10.1016/J.IJHYDENE.2019.04.041.
Kollmann, R., Neugebauer, G., Kretschmer, F., Truger, B., Kindermann, H., Stoeglehner, G., Ertl, T., Narodoslawsky, M., 2017. Renewable energy from wastewater - Practical aspects of integrating a wastewater treatment plant into local energy supply concepts. J. Clean. Prod. 155, 119–129. https://doi.org/10.1016/j.jclepro.2016.08.168.
Kumar, R., Singh, L., Wahid, Z.A., Din, M.F.M., 2015. Exoelectrogens in microbial fuel cells toward bioelectricity generation: a review. Int. J. Energy Res. https://doi.org/10.1002/er.3305.
Kundu, A., Sahu, J.N., Redzwan, G., Hashim, M.A., 2013. An overview of cathode material and catalysts suitable for generating hydrogen in microbial electrolysis cell. Int. J. Hydrogen. Energy. https://doi.org/10.1016/j.ijhydene.2012.11.031.
Liu, H., Grot, S., Logan, B.E., 2005. Electrochemically assisted microbial production of hydrogen from acetate. Environ. Sci. Technol. 39, 4317–4320. https://doi.org/10.1021/es050244p.
Logan, B.E., 2008. Microbial Fuel Cells. Microbial Fuel Cells 1–200. https://doi.org/10.1002/9780470258590.
Logan, B.E., Regan, J.M., 2006. Electricity-producing bacterial communities in microbial fuel cells. Trends. Microbiol. https://doi.org/10.1016/j.tim.2006.10.003.
Lu, L., Hou, D., Fang, Y., Huang, Y., Ren, Z.J., 2016. Nickel based catalysts for highly efficient H2 evolution from wastewater in microbial electrolysis cells. Electrochim. Acta 206, 381–387. https://doi.org/10.1016/J.ELECTACTA.2016.04.167.
Mahadevan, S., Erfle, J.D., Sauer, F.D., 1980. Degradation of soluble and insoluble proteins by bacteroides amylophilus protease and by rumen microorganisms. J. Anim. Sci. 50, 723–728. https://doi.org/10.2527/JAS1980.504723X.
Montpart, N., Rago, L., Baeza, J.A., Guisasola, A., 2015. Hydrogen production in single chamber microbial electrolysis cells with different complex substrates. Water. Res. 68, 601–615. https://doi.org/10.1016/j.watres.2014.10.026.
Obileke, K.C., Nwokolo, N., Makaka, G., Mukumba, P., Onyeaka, H., 2021. Anaerobic digestion: technology for biogas production as a source of renewable energy—A review. Energy Environ. https://doi.org/10.1177/0958305X20923117.
Paraskeva, P., Diamadopoulos, E., 2006. Technologies for olive mill wastewater (OMW) treatment: a review. J. Chem. Technol. Biotechnol. 81, 1475–1485. https://doi.org/10.1002/jctb.1553.
Postgate, J.R., Campbell, L.L., 1966. Classification of Desulfovibrio species, the nonsporulating sulfate-reducing bacteria. Bacteriol. Rev. 30, 732–738. https://doi.org/10.1128/br.30.4.732-738.1966.
Rashid, M., Khaloofah, M., Mesfer, A., Naseem, H., Danish, M., Al Mesfer, M.K., 2015. Hydrogen production by water electrolysis: a review of alkaline water electrolysis, PEM water electrolysis and high temperature water electrolysis. Int. J. Eng. Adv. Technol. (IJEAT).
Rosenblueth, M., Martínez, L., Silva, J., Martínez-Romero, E., 2004. Klebsiella variicola, a novel species with clinical and plant-associated isolates. Syst. Appl. Microbiol. 27 (1), 27–35. https://doi.org/10.1078/0723-2020-00261.
Rossi, R., Wang, X., Logan, B.E., 2020. High performance flow through microbial fuel cells with anion exchange membrane. J. Power. Sources. 475 https://doi.org/10.1016/j.jpowsour.2020.228633.
Rousseau, R., Etcheverry, L., Roubaud, E., Basséguy, R., Délia, M.L., Bergel, A., 2020. Microbial electrolysis cell (MEC): strengths, weaknesses and research needs from electrochemical engineering standpoint. Appl. Energy. https://doi.org/10.1016/j.apenergy.2019.113938.
Ruiz, Y., Baeza, J.A., Guisasola, A., 2013. Revealing the proliferation of hydrogen scavengers in a single-chamber microbial electrolysis cell using electron balances. Int. J. Hydrogen. Energy 38, 15917–15927. https://doi.org/10.1016/j.ijhydene.2013.10.034.
Selembo, P.A., Merrill, M.D., Logan, B.E., 2010. Hydrogen production with nickel powder cathode catalysts in microbial electrolysis cells. Int. J. Hydrogen. Energy 35, 428–437. https://doi.org/10.1016/j.ijhydene.2009.11.014.
Selembo, P.A., Merrill, M.D., Logan, B.E., 2009. The use of stainless steel and nickel alloys as low-cost cathodes in microbial electrolysis cells. J. Power. Sources. 190, 271–278. https://doi.org/10.1016/j.jpowsour.2008.12.144.
Singh, V., Das, D., 2019. Potential of hydrogen production from biomass. Science and Engineering of Hydrogen-Based Energy Technologies: Hydrogen Production and Practical Applications in Energy Generation 123–164. https://doi.org/10.1016/B978-0-12-814251-6.00003-4.
Sleutels, T.H.J.A., Hamelers, H.V.M., Rozendal, R.A., Buisman, C.J.N., 2009a. Ion transport resistance in Microbial Electrolysis Cells with anion and cation exchange membranes. Int. J. Hydrogen. Energy 34, 3612–3620. https://doi.org/10.1016/j.ijhydene.2009.03.004.
Sleutels, T.H.J.A., Lodder, R., Hamelers, H.V.M., Buisman, C.J.N., 2009b. Improved performance of porous bio-anodes in microbial electrolysis cells by enhancing mass and charge transport. Int. J. Hydrogen. Energy 34, 9655–9661. https://doi.org/10.1016/j.ijhydene.2009.09.089.
Tchobanoglous, G., Stensel, H.D., Tsuchihashi, R., Burton, F., Abu-Orf, M., Bowden, G., Pfrang, W., 2014. Metcalf & eddy. wastewater engineering. Treatment and Resource Recovery, 5th ed. McGray-Hill Education.
Valta, K., Kosanovic, T., Malamis, D., Moustakas, K., Loizidou, M., 2015. Overview of water usage and wastewater management in the food and beverage industry. Desalination Water Treat. 53, 3335–3347. https://doi.org/10.1080/19443994.2014.934100.
Walker, G., 2001. COD removal from textile industry effluent: pilot plant studies. Chem. Eng. J. 84, 125–131. https://doi.org/10.1016/S1385-8947(01)00197-8.
Wang, A., Liu, L., Sun, D., Ren, N., Lee, D.J., 2010. Isolation of Fe(III)-reducing fermentative bacterium Bacteroides sp. W7 in the anode suspension of a microbial electrolysis cell (MEC). Int. J. Hydrogen. Energy 35, 3178–3182. https://doi.org/10.1016/j.ijhydene.2009.12.154.
Watanabe, Y., Nagai, F., Morotomi, M., Sakon, H., Tanaka, R., 2010. Bacteroides clarus sp. nov., Bacteroides fluxus sp. nov. and Bacteroides oleiciplenus sp. nov., isolated from human faeces. Int. J. Syst. Evol. Microbiol. 60, 1864–1869. https://doi.org/10.1099/ijs.0.015107-0.
Younas, M., Shafique, S., Hafeez, A., Javed, F., Rehman, F., 2022. An overview of hydrogen production: current status, potential, and challenges. Fuel. https://doi.org/10.1016/j.fuel.2022.123317.
Zhang, Y., Merrill, M.D., Logan, B.E., 2010. The use and optimization of stainless steel mesh cathodes in microbial electrolysis cells. Int. J. Hydrogen. Energy 35, 12020–12028. https://doi.org/10.1016/j.ijhydene.2010.08.064.